Research Article Vol. 63, No. 1 / 1 January 2024 / Applied Optics 49

applied optics

Evolution of coherence singularities in polarization singular beams

Stuti Joshi,[1,2] Saba N. Khan,[1,3,*] and P. Senthilkumaran[1,4]

[1]Department of Physics, Indian Institute of Technology Delhi, Hauz Khas, New Delhi 110016, India
[2]Department of Optics, Palacký University, 17. Listopadu 12, 771 46 Olomouc, Czech Republic
[3]School of Physics and Astronomy, University of St. Andrews, North Haugh, St. Andrews KY16 9SS, UK
[4]Optics and Photonics Centre, Indian Institute of Technology Delhi, Hauz Khas, New Delhi 110016, India
*sabaphotonics@gmail.com

Received 27 September 2023; revised 22 November 2023; accepted 22 November 2023; posted 28 November 2023; published 21 December 2023

The evolution of correlation singularities in partially coherent polarization singular beams (PC-PSBs) is investigated. Since PSBs are the superposition of two orthogonally polarized vortex beams, the occurrence of coherence singularities in PC-PSBs is strongly governed by the topological charge of the component vortex beams and the spatial coherence length. Coherence singularities appear in the form of ring dislocations in the modulus of the spectral degree of coherence (SDoC) profile, and the number of ring dislocations is equal to the higher value of the topological charge of the superposing vortex beam. Furthermore, the SDoC phase profile can be used to determine the polarity of a PC-PSB. The findings of the study could be valuable in various applications that rely on the spatial coherence of beams, such as free-space communication and imaging.

https://doi.org/10.1364/AO.506815

1. INTRODUCTION

Singular optics deals with the effects that occur near a singular point where some parameter of the optical field is not defined. Exploring singularities in an electromagnetic wave field has remained a mainstay in the past few decades [1–3]. The most commonly discussed singularity in electromagnetic fields is the phase singularity. Also known as a vortex beam, it carries orbital angular momentum (OAM). The orthogonally polarized vortex beams with distinct OAM content combine to yield yet another form of electromagnetic singularity called a "polarization singularity." Point polarization singularities are classified into two types, namely, vector field (V-point) and ellipse field (C-point) singularities [1,2]. The beams that carry a polarization singularity at the core are referred to as polarization singular beams (PSBs). PSBs can be identified as polarization azimuth vortices found within the Stokes phase distribution $\Phi_{12} = \mathrm{Arg}\{S_1 + iS_2\}$ (where S_1 and S_2 represent the Stokes parameters). In analogy with the topological charge ($m = \frac{1}{2\pi}\oint \nabla\chi \cdot dl$), which depicts the strength of the phase gradient ($\nabla\chi$) of the vortex beams, the Stokes index ($\sigma_{12} = \frac{1}{\pi}\oint \nabla\gamma \cdot dl$) is used to determine the strength of the azimuth gradient ($\nabla\gamma$) around the singularity for the PSBs. Furthermore, the Stokes index is connected to the C-point index I_c and the V-point index η as $2I_c = \sigma_{12}$ and $2\eta = \sigma_{12}$, respectively. In recent years, PSBs have attracted a great deal of interest due to their potential applications in optical trapping and manipulation [4], propagation through atmospheric turbulence [5], edge enhancement [2], high-dimensional quantum key distribution [6], weak field measurement [7], etc.

The above-discussed phase singularities and polarization singularities occur in coherent vortex wave fields with deterministic two-point correlation. It is demonstrated that the phase singularity of the vortex beam disappears when the spatial coherence is reduced as the dark core is filled with diffused light [3]. In such partially coherent systems, these disappeared phase singularities emerge as another type of electromagnetic singularity called the "coherence singularity" [3,8–10]. Coherence singularities occur at a pair of points where the modulus of the spectral degree of coherence (SDoC) becomes zero and its phase is undetermined. The robustness of the coherence singularities makes them a useful candidate for free-space communication. Moreover, coherence singularities prove to be beneficial in determining both the magnitude and polarity of vortex beams under extremely low-coherence conditions, when the beam loses its distinctive features of intensity and phase distribution [3,11]. The investigation of correlation singularities is also extended to the partially coherent beams with a multi-Gaussian correlation function. A straightforward relationship has been identified, indicating that the number of ring dislocations is M-1, where M is the beam index of multi-Gaussian Schell model beams [12].

Partially coherent (PC) beams are advantageous in many applications such as imaging [13], free-space optical communication [14], particle trapping [15], optical encryption [16], beam shaping [17], and optical image transmission [18]. Substantial overlap between the applications of PC beams and PSBs initiated the investigation of the statistical properties of partially coherent PSBs (PC-PSBs) [19–22] to harness the two-fold benefit of spatial correlation and inhomogeneous polarization.

Recently, the three different ways of characterizing the singularities of a partially coherent electromagnetic wavefield have been discussed [23]. Although our previous study briefly mentioned the presence of coherence singularities in V-point beams [21], a comprehensive exploration of coherence singularities in PC-PSBs has not been conducted to date. This manuscript presents the first-ever investigation of the complete evolution of coherence singularities in PC-PSBs. Coherence singularities in PC-PSBs are strongly governed by the OAM content of the superposing beams and the spatial coherence length. These singularities appear in the form of ring dislocations in the modulus of the SDoC profile. The finding indicates that as the spatial coherence decreases, the phase singularities (point dislocations) present in the superposing vortex beams transform into coherence singularities (ring dislocations). However, the polarization singularity remains intact.

2. EVOLUTION OF COHERENCE SINGULARITIES IN PC-PSBs

A. Theoretical Background

We consider that the PC-PSBs are generated from a quasi-monochromatic Gaussian Schell-model type input beam of beam waist w and coherence length δ. The statistical behavior of the fluctuating fields is described by a cross-spectral density matrix (CSD). The elements of the CSD matrix of a PC-PSB at the source are given by [20]

$$W_{0xx/0yy}(\mathbf{r}_1;\mathbf{r}_2) = [\pm \mathbf{r}_1^{|m_1|} e^{im_1\phi_1} + \mathbf{r}_1^{|m_2|} e^{-i(m_2\phi_1+\theta_0)}] \\ [\pm \mathbf{r}_2^{|m_1|} e^{-im_1\phi_2} + \mathbf{r}_2^{|m_2|} e^{i(m_2\phi_2+\theta_0)}]\mu(\mathbf{r}_1,\mathbf{r}_2), \tag{1a}$$

$$W_{0xy/0yx}(\mathbf{r}_1;\mathbf{r}_2) = \mp i[\pm \mathbf{r}_1^{|m_1|} e^{im_1\phi_1} + \mathbf{r}_1^{|m_2|} e^{-i(m_2\phi_1+\theta_0)}] \\ [\mp \mathbf{r}_2^{|m_1|} e^{-im_1\phi_2} + \mathbf{r}_2^{|m_2|} e^{i(m_2\phi_2+\theta_0)}]\mu(\mathbf{r}_1,\mathbf{r}_2), \tag{1b}$$

where $\mu(\mathbf{r}_1,\mathbf{r}_2) = \exp(-\frac{r_1^2+r_2^2}{w^2}) \exp(-\frac{r_1^2+r_2^2-2r_1r_2\cos(\phi_1-\phi_2)}{2\delta^2})$, and $\mathbf{r}_1(r_1,\phi_1)$ and $\mathbf{r}_2(r_2,\phi_2)$ correspond to two points in the source plane. The frequency dependence is omitted for a quasi-monochromatic field. Here, $(m_1;m_2)$ and $(\phi_1;\phi_2)$ represent topological charges and azimuthal phases of the superposing vortex beams, respectively. The elements of the CSD matrix for a pair of inhomogeneously polarized orthogonal beams can be obtained by substituting $\theta_0 = 0$ (positive polarity) and π (negative polarity) [21]. The beam exhibits a V-point singularity when $|m_1| = |m_2|$ and a C-point singularity when $|m_1| \neq |m_2|$(as shown in Fig. 1). If either m_1 or m_2 equals zero, the resulting beam takes the form of a bright C-point beam (indicated by a blue outline in Fig. 1), while otherwise, it becomes a dark C-point beam (outlined in yellow in Fig. 1) [2]. It is worth mentioning that the plotting of the SoP distribution does not take into account the weighted intensity dependence. We have considered PC-PSBs with $I_c = \pm\frac{1}{2}, \pm1, \pm2$ and $\eta = \pm1, \pm2$ for our study.

The CSD matrix ($\mathbf{W}(\boldsymbol{\rho}_1,\boldsymbol{\rho}_2,z)$) elements at the observation plane can be calculated using the generalized Collins formula [24]

$$W_{\alpha\beta}(\boldsymbol{\rho}_1,\boldsymbol{\rho}_2,z) = \frac{k^2}{4\pi^2B^2}\int_0^{2\pi}\int_0^{2\pi}\int_0^{\infty}\int_0^{\infty} r_1r_2\mathrm{d}r_1\mathrm{d}r_2\mathrm{d}\phi_1\mathrm{d}\phi_2 \\ \times W_{0\alpha\beta}(\mathbf{r}_1,\mathbf{r}_2)\exp\left[\frac{ikD}{2B}(\rho_2^2-\rho_1^2) - \frac{ikA}{2B}(r_1^2-r_2^2)\right] \\ \times \exp\left[\frac{ik}{B}(r_1\rho_1\cos(\theta_1-\phi_1) - r_2\rho_2\cos(\theta_2-\phi_2))\right], \tag{2}$$

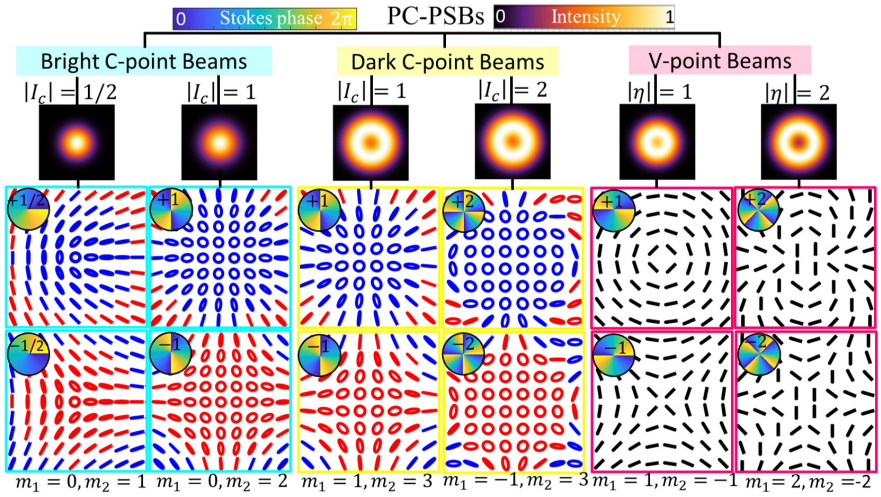

Fig. 1. Schematic showing a general classification of polarization singular beams. (top) Spectral density profiles and (bottom) SoP distributions with embedded Stokes phase profiles.. Here, $\delta = 4$ mm. The intensity profile is degenerate for both positive and negative index PC-PSBs; however, the Stokes phases and SOPs differentiate them. The SoP distribution plot does not take into account the weighted intensity dependence.

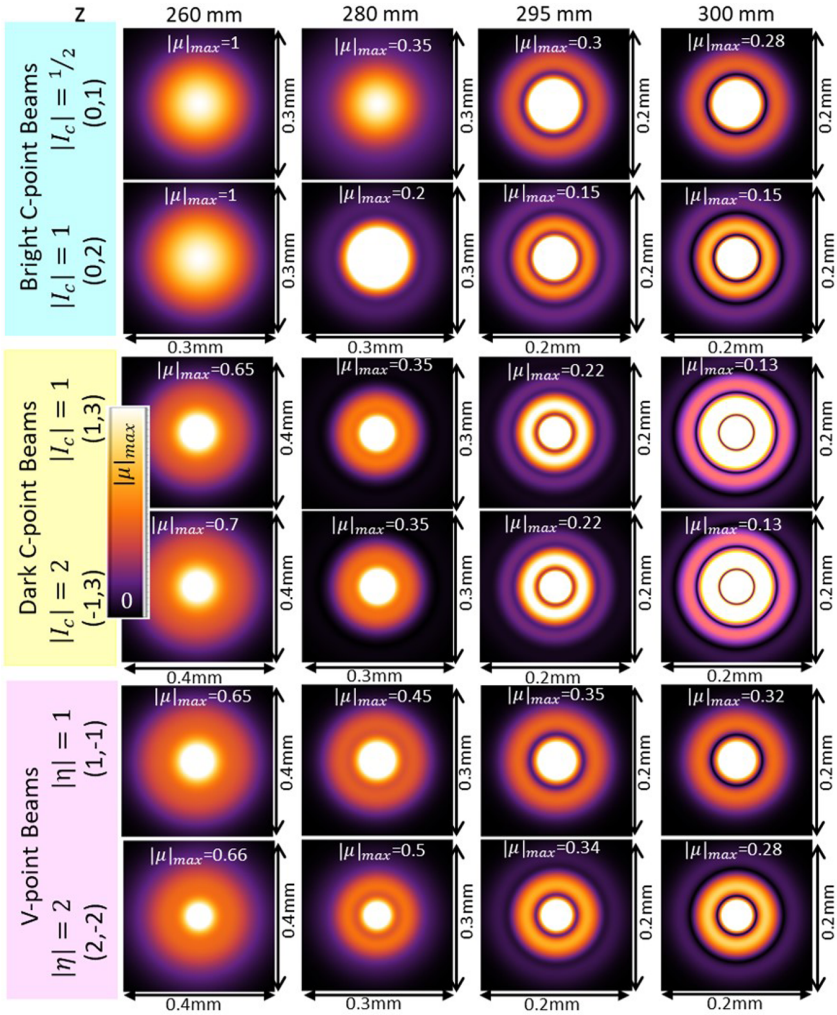

Fig. 2. Evolution of coherence singularities in the modulus of the SDoCs for various PC-PSBs ($\delta = 0.5$ mm). The singularity evolves in the form of ring dislocations, and the number of ring dislocations is equal to the higher value of the topological charge of the superposing beam. Different scale bars are used for these distributions, each of which is indicated alongside its corresponding SDoC pattern.

where $(\alpha; \beta) = (x, y)$; k is a propagation constant, and $\boldsymbol{\rho}_1(\rho_1, \theta_1)$ and $\boldsymbol{\rho}_2(\rho_2, \theta_2)$ are two transverse points in the observation plane. A $2f$ lens system is considered to study the propagation properties, and the lens plane is assumed to be the $z = 0$ plane. Therefore, the transfer matrix elements are $A = (1 - z/f)$, $B = f$, $C = -1/f$, and $D = 0$.

The spectral density of a PC-PSB can be evaluated as [25]

$$S(\boldsymbol{\rho}) = \mathrm{Tr}[\mathbf{W}(\boldsymbol{\rho}, \boldsymbol{\rho}, z)]. \tag{3}$$

Figure 1 depicts the presence of bright C-point, dark C-point, and V-point singularities in the state of polarization (SoP) distribution of PC-PSBs at the focal plane. The beam parameters are $\lambda = 632.8$ nm, $w = 2.5$ mm, $\delta = 4$ mm, and $f = 300$ mm. The spectral density profiles of V-point and dark C-point PC-PSBs exhibit doughnut-shaped profiles, while bright C-point PC-PSBs have flat-top/Gaussian profiles. For a specific combination of superposing vortex beams (m_1, m_2), the spectral density profile of the resulting PSBs (type-I, II, III, IV) is indistinguishable for both positive $(\theta = 0)$ and negative $(\theta = \pi)$ polarities. However, the SoP distribution distinguishes its type [21]. It is demonstrated that for the low value of spatial coherence, different index PC-PSBs exhibit similar Gaussian intensity profiles due to the coherence-induced depolarization effect [21,26]. However, the polarization vortices (SoP distribution) remain intact. At this point, it would be interesting to see how source spatial coherence affects the coherence properties of the PC-PSBs at the observation plane.

For a spatially partially coherent beam, the extent of correlation between two spatial points is characterized by the spectral degree of coherence as [25]

$$\mu(\boldsymbol{\rho}_1, \boldsymbol{\rho}_2, z) = \frac{\mathrm{Tr}\mathbf{W}(\boldsymbol{\rho}_1, \boldsymbol{\rho}_2, z)}{\sqrt{S(\boldsymbol{\rho}_1, z) S(\boldsymbol{\rho}_2, z)}}. \tag{4}$$

Here, $S(\boldsymbol{\rho}_j, z)$; $(j = 1, 2)$ represents the spectral density. SDoC is a complex quantity with $0 \le |\mu(\boldsymbol{\rho}_1, \boldsymbol{\rho}_2, z)| \le 1$. The extreme values of zero and one represent the complete absence and presence of correlation of the fields at a pair of points $(\boldsymbol{\rho}_1,$

$\boldsymbol{\rho}_2$), respectively. It is well established that the coherence singularities occur when the phase of the SDoC is undefined, i.e., $|\mu(\boldsymbol{\rho}_1, \boldsymbol{\rho}_2, z)| = 0$ [8]. The simultaneous occurrence of the zeroes of the real and imaginary parts of the numerator of Eq. (4) ($\mathrm{Tr}[\mathbf{W}(\boldsymbol{\rho}_1, \boldsymbol{\rho}_2, z)]$) determines the locations of the coherence singularities

$$\mathrm{Re}[\mathrm{Tr}(\mathbf{W})(\boldsymbol{\rho}_1, \boldsymbol{\rho}_2, z)] = 0, \quad \text{and} \quad \mathrm{Im}[\mathrm{Tr}(\mathbf{W})(\boldsymbol{\rho}_1, \boldsymbol{\rho}_2, z)] = 0. \tag{5}$$

It is evident from Eqs. (1), (2), and (4) that the SDoC distribution depends upon the source parameters (m_1, m_2, δ) and the propagation distance (z). In order to understand how the coherence singularities in the PC-PSBs come into existence, we first study the propagation properties of SDoC. To achieve this, we numerically solved the integration, and the numerical outcomes illustrating the evolution of coherence singularities in SDoC distributions for different PC-PSBs are depicted in Fig. 2 (with δ set at 0.5 mm). Here, one of the spatial points in the observation plane is kept fixed at the origin ($\boldsymbol{\rho}_1 = 0$). At the source plane, various PC-PSBs exhibit similar Gaussian distribution in the modulus of SDoC [Eq. (1)], which undergoes a transformation into a non-Gaussian profile as the beam

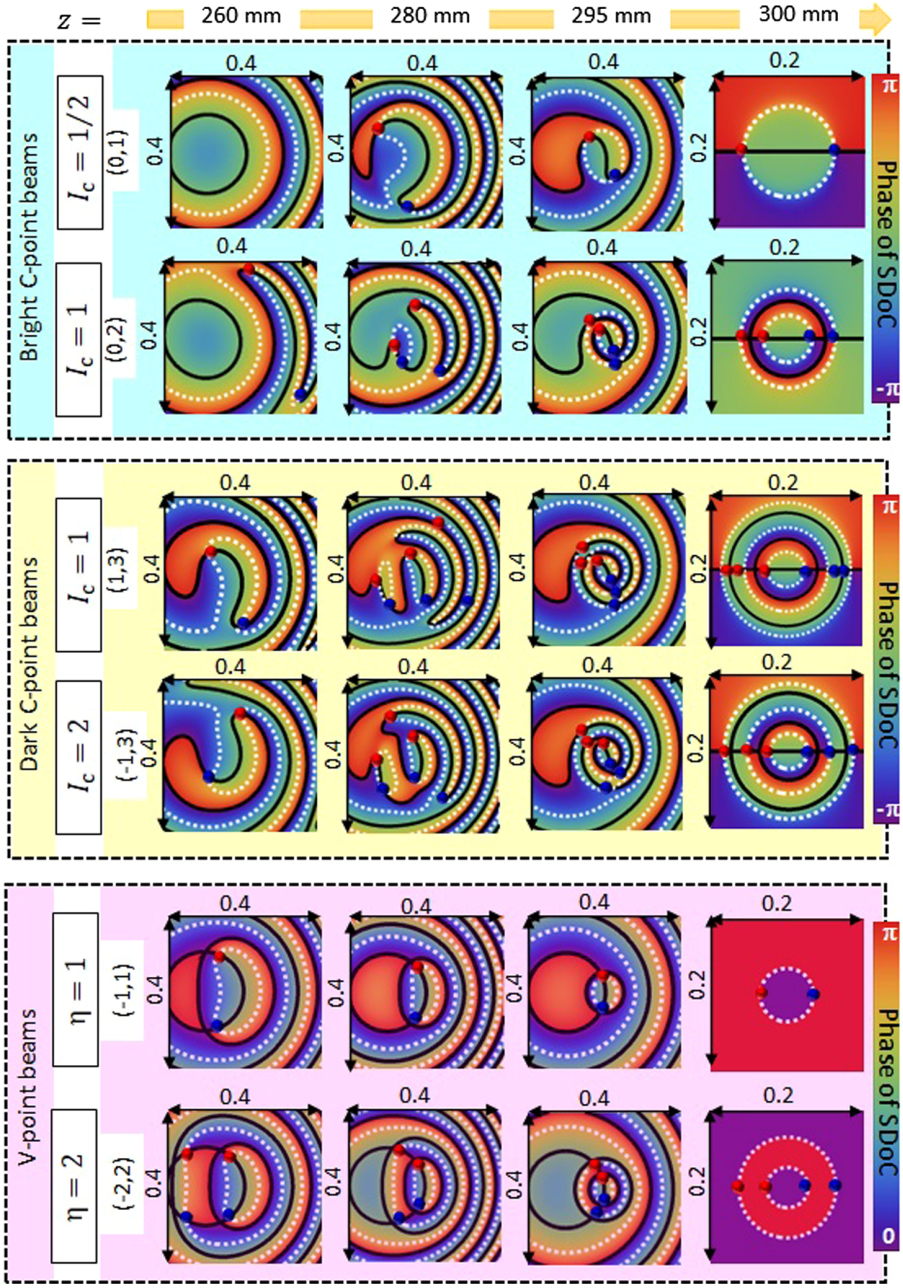

Fig. 3. SDoC phase profile along with the real (white contour line) and imaginary (black contour line) parts of $\mathrm{Tr}\mathbf{W}(\boldsymbol{\rho}, z)$ for various PC-PSBs at different propagation distances for $\delta = 0.5$ mm. Coherence singularities are located at the point of intersections of real and imaginary parts of the $\mathrm{Tr}[\mathbf{W}(\boldsymbol{\rho}_1, \boldsymbol{\rho}_2, z)]$. The positive and negative singularities are shown with blue and red spheres, respectively. Distinct window sizes are used for the evolving observation plane and the focal plane.

propagates. When $z = 260$ mm, the coherence singularity starts appearing in V-point beams in the form of ring dislocations, and its strength increases gradually as the beam approaches the focal plane.

B. Results and Discussion

It is observed that the number of ring dislocations (n) in the SDoC distribution of the PC-PSB is governed by the topological charges of the superposing beams (m_1, m_2). Since bright C-point PSBs are the combination of a Gaussian beam ($m_1 = 0$) and a vortex beam (m_2), the number of ring dislocations is equivalent to the topological charge of the vortex beam ($n = |m_2|$). This aspect can be readily used to determine the polarization singularity index of the PC bright C-point beams ($|I_c| = n/2$). The evolution of coherence singularities on propagation is the result of the conversion of phase singularities into coherence singularities [3]. Partially coherent V-point beams are composed of two orthogonally polarized vortex beams having equal and opposite topological charges ($|m_1| = -|m_2|$), and the number of ring dislocations is equal to the topological charge of the vortex beams ($n = |m_1| = |m_2|$). In these cases, the coherence singularity of the superposing states always coexists in the SDoC distributions such that $|\eta| = n$. Interestingly, for PC dark C-point beams the number of ring dislocations is equal to the higher value of the topological charge of the superposing beam irrespective of their $|I_c|$ index. For example, dark C-point beams having $|I_c| = 1$ ($m_1 = 1$, $m_2 = 3$) and $|I_c| = 2$ ($m_1 = -1$, $m_2 = 3$) possess three ring dislocations in the SDoC distributions. The ring dislocations are the consequence of the coexistence of the coherence singularities of the superposing vortex beams. In contrast to the intensity profile, which shows an expanding dark core radius (high δ), the SDoC profile demonstrates an increasing number of rings (low δ) with the increase in charge of the superimposed beams (m_1 or $m_2 \neq 0$). Consequently, PC-PSBs comprising states with higher charges exhibit inner rings with smaller radii.

To analyze the occurrence of coherence singularities in PC-PSBs, we have plotted the real (white) and imaginary (black) parts of the cross-spectral density in Fig. 3. The phase of the SDoC distribution was determined using an off-axis reference point, $\boldsymbol{\rho}_1(\rho_{1x} = 0.1\ \text{mm}, \rho_{1y} = 0)$ while other parameters remained consistent with Fig. 2. The coherence singularity appears at the locations where the contour lines of real and

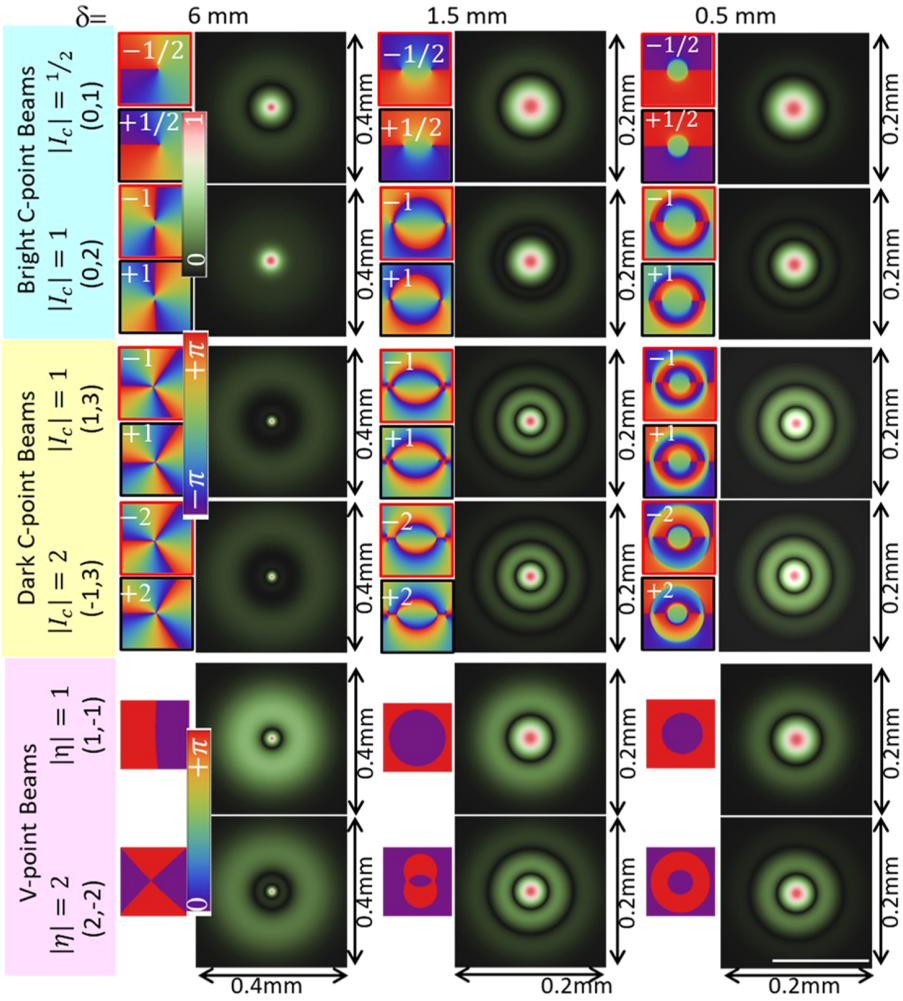

Fig. 4. Modulus and phase of SDoC for various PC-PSBs at $z = f$ for different values δ. The SDoC profile is degenerate for a particular PC-PSB while the SDoC phase distinguishes the polarity/type. The computation window for higher coherence lengths ($\delta = 6$ mm) is 0.4 mm × 0.4 mm, and for lower coherence lengths ($\delta = 1.5$ mm and 0.5 mm) is 0.2 mm × 0.2 mm.

imaginary parts of the CSD intersect each other. When the propagation distance is $z < 260$ mm there are no correlation singularities around the center. It can be seen that the coherence singularities in the phase distribution of the SDoC appear as point dislocations for $z > 260$ mm. Positive and negative coherence singularities correspond to the SDoC-phase rotating in the anticlockwise ($-\pi$ to π) and clockwise (π to $-\pi$) directions, respectively. It is observed that the coherence singularities always appear as a pair that contains positive (blue spheres) and negative (red spheres) polarity coherence singularities. These paired singularities undergo rotation during propagation and eventually align along a line in the focal plane. In our case, the coherence singularities move along a horizontal line due to the choice of the reference point ($\boldsymbol{\rho}_1 = 0$). The number of point singularities in the SDoC phase distribution is two times the number of ring dislocations due to the off-axis displacement of the reference point. Like the partially coherent vortex beam [10], the coherence singularities in PC-PSBs evolve in a van-Cittert Zernike manner on propagation, devoid of any coherence singularity at the source plane. Interestingly, in the far field, the point dislocations convert into edge dislocations, as depicted with the steplike jump in the SDoC phase distribution.

It is clear from the previous discussion that the complete evolution of coherence singularity takes place in the far field. Next, we study the behavior of coherence singularities by varying the source spatial coherence length at the focal plane as depicted in Fig. 4. Coherence singularities are prominently seen for low spatial coherence length (1.5 mm and 0.5 mm) compared to higher values (6 mm). The changes observed in the SDoC (modulus and phase) on reducing spatial coherence are similar to the effects observed during the propagation, i.e., conversion of phase singularity into coherence singularity. Analogous to the spectral density of positive and negative polarity of a particular PC-PSB, the modulus of the SDoC is also degenerate. However, one can predict the polarity of a particular index of the PC-PSBs from the SDoC phase profile.

3. CONCLUSION

The evolution of the coherence singularities in PC-PSBs is investigated. It is observed that the coherence singularities strongly depend on the coherence length and topological charges of the component vortex beams. Coherence singularities in PC-PSBs appear as ring dislocations in the modulus of the SDoC profile (at $z = f$). The dark rings of the superposing states coexist in the SDoC profile. The number of ring dislocations of the PC-PSBs is equal to the higher value of the topological charge of the component vortex beam. These ring dislocations can be used to predict the magnitude of the polarization singularity index of the V-point ($|\eta| = n$) and bright C-point ($|I_c| = n/2$) PC-PSBs. Since the I_c-index of the dark C-point beam is shared by infinitely many combinations of superposing OAM states ($I_c = (m_2 - m_1)/2$), the number of ring dislocations is not sufficient to determine the $|I_c|$-index. The SDoC phase distribution can be used to determine the polarity/type of PC-PSBs. On reducing the spatial coherence the phase singularities (point dislocations) present in the superposing vortex beams convert into coherence singularities (ring dislocations) while the polarization singularity in PC-PSBs remains intact. Recent studies have indicated the potential of PSBs in free-space optical communication and high-dimensional quantum key distribution. Consequently, gaining a deeper understanding of the coherence properties of PC-PSBs becomes valuable, as it may facilitate the future incorporation of partial coherence in these applications.

Disclosures. The authors declare no conflicts of interest.

Data availability. Data underlying the results presented in this paper are not publicly available at this time but may be obtained from the authors upon reasonable request.

REFERENCES

1. M. Dennis, "Polarization singularities in paraxial vector fields: morphology and statistics," Opt. Commun. **213**, 201–221 (2002).
2. P. Senthilkumaran, *Singularities in Physics and Engineering* (IOP Publishing, 2018).
3. X. Liu, J. Zeng, and Y. Cai, "Review on vortex beams with low spatial coherence," Adv. Phys. X **4**, 1626766 (2019).
4. Q. Zhan, "Trapping metallic Rayleigh particles with radial polarization: reply to comment," Opt. Express **20**, 6058–6059 (2012).
5. K. Khare, P. Lochab, and P. Senthilkumaran, *Orbital Angular Momentum States of Light* (IOP Publishing, 2020), pp. 2053–2563.
6. A. Forbes and I. Nape, "Quantum mechanics with patterns of light: progress in high dimensional and multidimensional entanglement with structured light," AVS Quantum Sci. **1**, 011701 (2019).
7. M. R. Dennis and J. B. Götte, "Topological aberration of optical vortex beams: determining dielectric interfaces by optical singularity shifts," Phys. Rev. Lett. **109**, 183903 (2012).
8. G. Gbur and T. D. Visser, "Coherence vortices in partially coherent beams," Opt. Commun. **222**, 117–125 (2003).
9. C. Stahl and G. Gbur, "Partially coherent vortex beams of arbitrary order," J. Opt. Soc. Am. A **34**, 1793–1799 (2017).
10. Y. Zhang, Y. Cai, and G. Gbur, "Partially coherent vortex beams of arbitrary radial order and a van Cittert-Zernike theorem for vortices," Phys. Rev. A **101**, 043812 (2020).
11. X. Lu, C. Zhao, Y. Shao, *et al.*, "Phase detection of coherence singularities and determination of the topological charge of a partially coherent vortex beam," Appl. Phys. Lett. **114**, 201106 (2019).
12. Y. Zhang, H. Wang, C. Ding, *et al.*, "Correlation singularities of partially coherent beams with multi-Gaussian correlation function," Phys. Lett. A **381**, 2550–2553 (2017).
13. J. M. Soto, J. A. Rodrigo, and T. Alieva, "Label-free quantitative 3d tomographic imaging for partially coherent light microscopy," Opt. Express **25**, 15699–15712 (2017).
14. O. Korotkova, "Scintillation index of a stochastic electromagnetic beam propagating in random media," Opt. Commun. **281**, 2342–2348 (2008).
15. M. Dong, D. Jiang, N. Luo, *et al.*, "Trapping two types of Rayleigh particles using a focused partially coherent anomalous vortex beam," Appl. Phys. B **125**, 55 (2019).
16. D. Peng, Z. Huang, Y. Liu, *et al.*, "Optical coherence encryption with structured random light," PhotoniX **2**, 1–15 (2021).
17. Y. Chen, F. Wang, and Y. Cai, "Partially coherent light beam shaping via complex spatial coherence structure engineering," Adv. Phys. X **7**, 2009742 (2022).
18. Y. Liu, X. Zhang, Z. Dong, *et al.*, "Robust far-field optical image transmission with structured random light beams," Phys. Rev. Appl. **17**, 024043 (2022).
19. J. Zeng, C. Liang, H. Wang, *et al.*, "Partially coherent radially polarized fractional vortex beam," Opt. Express **28**, 11493–11513 (2020).
20. S. N. Khan, S. Joshi, and P. Senthilkumaran, "Coherence-induced depolarization effects in polarization singular beams," Opt. Lett. **47**, 6448–6451 (2022).
21. S. Joshi, S. N. Khan, P. Senthilkumaran, *et al.*, "Statistical properties of partially coherent polarization singular vector beams," Phys. Rev. A **103**, 053502 (2021).

22. Y. Zhang, Y. Cui, F. Wang, *et al.*, "Correlation singularities in a partially coherent electromagnetic beam with initially radial polarization," Opt. Express **23**, 11483–11492 (2015).
23. W. S. Raburn and G. Gbur, "Singularities of partially polarized vortex beams," Front. Phys. **8**, 168 (2020).
24. Q. Lin and Y. Cai, "Tensor ABCD law for partially coherent twisted anisotropic Gaussian–Schell model beams," Opt. Lett. **27**, 216–218 (2002).
25. E. Wolf, *Introduction to the Theory of Coherence and Polarization of Light* (Cambridge University, 2007).
26. S. Joshi, S. N. Khan, Manisha, *et al.*, "Coherence-induced polarization effects in vector vortex beams," Opt. Lett. **45**, 4815–4818 (2020).